Advanced Ceramics Progress: Vol. 7, No. 2, (Spring 2021) 34-43

Materials and Energy Research Center
MERC

Contents lists available at ACERP

Advanced Ceramics Progress

Journal Homepage: www.acerp.ir

Original Research Article

Optical Properties and Crystallization Behavior of SiO_2-Al_2O_3-BaO-BaF_2 Glasses Containing Different Amounts of Bi_2O_3

A. Ahmadi Kordlar [a], M. Rezvani [b] *

[a] *MS, Department of Materials Engineering, Faculty of Mechanical Engineering, University of Tabriz, Tabriz, East Azerbaijan, Iran*
[b] *Professor, Department of Materials Engineering, Faculty of Mechanical Engineering, University of Tabriz, Tabriz, East Azerbaijan, Iran*

ARTICLE INFO

Article History:

Received 24 May 2021
Received in revised form 14 July 2021
Accepted 10 August 2021

Keywords:

Optical Glass
Oxy-Fluoride
BaF_2
Bi_2O_3

ABSTRACT

The present study aims to investigate the optical properties and crystallization behavior of oxy-fluoride glasses with different amounts of Bi_2O_3. Glasses with compositions of $45SiO_2$-$15Al_2O_3$-25BaO-$15BaF_2$-xBi_2O_3 (x=0, 1, 2.5, 4, and 6) (mole ratio) were prepared using melt-quenching method. Owing to the network modifying role of Bi_2O_3 and increasing number of Non-Bridging Oxygens (NBOs), the molar volume increased from 27.69 to 31.60 cm^3 and microhardness was reduced from 720.21 to 613.10 MPa. In order to study the structural changes, the FTIR spectra were recorded, and increment of NBOs by adding Bi_2O_3 as well as the presence of Bi° particles in the sample containing six mole ratios of Bi_2O_3 were proved. The UV-Vis transmittance spectra were employed to determine the optical properties including Fermi energy, direct and indirect optical band gaps, and Urbach energy. The Fermi energy and optical band gaps were reduced as the Bi_2O_3 content increased. The degree of structural disorderliness (Urbach energy) increased from 0.170 to 0.212 eV followed by creating more NBOs through Bi_2O_3 addition. On the basis of UV-Vis-IR transmittance results, the sample containing four mole ratios of Bi_2O_3 exhibited the highest transmittance in IR region and its IR cut-off shifted to longer wavelengths. Further, the sample with six mole ratios of Bi_2O_3 was characterized as the highest refractive index (1.7) among other glasses. Finally, evaluation of crystallization behavior of specimens revealed that it was impossible to prepare transparent glass ceramics containing BaF_2 nanocrystals due to the surface crystallization in these glasses.

https://doi.org/10.30501/ACP.2021.287637.1063

1. INTRODUCTION

Rare-earth-doped transparent glasses and glass ceramics are important materials with many applications in photonics such as optical fibers, laser host materials, up-conversion lasers, amplifiers, and three-dimensional displays [1-3]. Although oxide glasses and glass ceramics are characterized by thermal, chemical, and mechanical durability, their high phonon energies (~1100 cm^{-1}) and limited solubility of rare-earth ions have restricted their optical applications [4-8]. On the contrary, apart from the low phonon energies (~500 cm^{-1}) of fluoride glasses, they suffer high devitrification rate during preparation as well as low chemical, mechanical, and thermal stability [9,10]. Since acceptable optical properties are not enough for an optical material, special efforts have been devoted to produce novel glasses based on both oxides and fluorides. Introduction of oxygen to fluoride glasses or addition of fluorine to oxide glasses increases their crystallization rates; however, it is revealed that oxygen can stabilize the amorphous state when added as specific oxides to fluoride melts [11]. Accordingly, these types of

* Corresponding Author Email: m_rezvani@tabrizu.ac.ir (M. Revani)
URL: https://www.acerp.ir/article_136414.html

Please cite this article as: Ahmadi Kordlar, A., Rezvani, M., "Optical Properties and Crystallization Behavior of SiO_2-Al_2O_3-BaO-BaF_2 Glasses Containing Different Amounts of Bi_2O_3", ***Advanced Ceramics Progress***, Vol. 7, No. 2, (2021), 34-43. https://doi.org/10.30501/ACP.2021.287637.1063

glasses, called oxy-fluoride glasses, were introduced which received considerable attention since they benefited from advantages of both fluoride and oxide glasses [11,12]. These new materials were considered as excellent hosts for rare-earth ions; however, the structural defects caused by the amorphous structure can entrap electrons and holes, thus resulting in non-radiative processes [13]. In order to solve this problem, oxy-fluoride glass ceramics were introduced and prepared by Wang and Ohwaki [14] for the first time. The precipitated crystalline phase in these glass ceramics was $Pb_xCd_{1-x}F_2$ nanocrystals, and the doped ions (Yb^{3+} and Er^{3+}) were preferably segregated from the glassy matrix to the crystalline phase [14]. Due to the environmental problems of PbF_2 and CdF_2, other oxy-fluoride systems were proposed [15]. Among the several already existing systems, the species with MF_2 (M= Ba, Ca, and Sr) nanocrystals have become of interest owing to their economical and non-toxic raw materials [16]. Furthermore, trivalent rare-earth ions could be substituted for the divalent alkaline-earth cations and lead to suitable solubility of rare-earth ions in MF_2 nanocrystals [17].

BaF_2 in its crystalline form exhibits lower phonon energy (~346 cm^{-1}) than crystalline CaF_2 (~466 cm^{-1}), and its IR cutoff is placed at longer wavelengths. Consequently, the IR window provided by BaF_2 is wider than CaF_2 [18,19]. Nevertheless, contrary to the oxy-fluoride glasses and glass ceramics containing CaF_2, there are only a few studies on optical properties of the aluminosilicate oxy-fluoride systems based on BaF_2 [5,20-23]. Therefore, the present study aims to evaluate the optical properties of new oxy-fluoride glasses of SiO_2-Al_2O_3-BaO-BaF_2 system in the presence of different amounts of Bi_2O_3 additive. The main reason why this additive has been used is the important role of Bi_2O_3 in increasing the refractive index of the glasses [24,25]. To the best of the author's knowledge, no report on its effects of the optical properties of oxy-fluoride glasses and glass ceramics has been found. In this regard, oxy-fluoride glasses with different contents of Bi_2O_3 were prepared using the melt-quenching method. Then, changes in the density, molar volumes, and microhardness of samples were studied. Structural changes and optical properties including transparency in UV-Vis-IR region, Fermi energy, direct and indirect band gap energies, Urbach tailing, and refractive index of glasses were also examined.

2. EXPERIMENTAL PROCEDURE

2.1. Materials, Sample Preparation, and Analyses

Oxy-fluoride glasses with chemical compositions of $45SiO_2$-$15Al_2O_3$-25BaO-$15BaF_2$-xBi_2O_3 (x=0, 1, 2.5, 4, and 6) (mole ratio) were prepared through the conventional melt-quenching method and they were nominated as GBi0, GBi1, GBi2.5, GBi4, and GBi6, respectively. The samples were obtained using high-purity materials such as Al_2O_3 (101077 Merck) and BaF_2 (202746 Sigma-Aldrich). In order to reach high-purity SiO_2 (approximately 99.5%), Hamedan silica was leached by HCl and calcined at 800 °C for 2 hours. $BaCO_3$ (513779 Uni-Chem) was also used to supply BaO.

In this respect, 30 g of batches were melted in covered alumina crucibles in an electric furnace at 1500 °C for one hour. The obtained melts were poured on stainless steel plates and then, they were pressed by another plate to produce disc-shaped glasses with the thickness of 3-5 mm. To relieve internal stresses, the shaped glasses were annealed at 500 °C for one hour and cooled to room temperature with a controlled cooling rate.

To investigate the crystallization behavior and determine the crystallization temperature of samples, Differential Scanning Calorimetry (DSC) was performed (NETZSCH STA 449 F3) at the heating rate of 10 °C/min. In addition, X-Ray Diffraction (XRD) patterns of glasses and crystallized samples were recorded (Philips Xpert MMD system) to identify the amorphous nature of glasses and precipitated crystalline phases in glass ceramics. Vickers microhardness of the glasses was obtained using HV-1000Z Technologies PACE instruments under the load of 1 N for 15 s. The FTIR spectra were recorded by FTIR Tensor 27 Brucker to assess the structural changes. Optical transmittance spectra of bulk glasses in the UV-Vis-IR range of wavelengths were achieved using UV-Vis-NIR Shimadzu 3100 and FTIR Shimadzu 8400S.

2.2. Calculation of Density and Molar Volume

Density (d) of a glass is calculated using Equation (1) with considering its weights in air (W_1) and water (W_2):

$$d = \frac{W_1}{W1\text{-}W_2} \quad (1)$$

Obviously, the relationship between molar volume (V_m) and density is defined by Equation (2), as shown in the following:

$$V_m = \sum \left(\frac{Mi}{d}\right) \quad (2)$$

where M_i is the molar mass of component "i" in glass and is equal to that in Equation (3):

$$M_i = C_i A_i \quad (3)$$

where C_i and A_i are the molar concentration and molecular weight of component "i", respectively.

2.3. UV-VIS Spectra and Optical Constants Measurements

2.3.1. Fermi Energy, Band Gap, and Urbach Tailing

For transparent glasses, Fermi energy level (E_F) is determined using the Fermi-Dirac distribution function (Equation (4)):

$$K(\lambda) = \frac{1}{1 + \exp(\frac{E_F - E}{k_B T})} \quad (4)$$

In Equation (4), E_F and E stand for Fermi energy and energy of the probing photon, respectively. In addition, k_B and K(λ) are Boltzmann constant and extinction coefficient, respectively. This equation can be written as follows:

$$k_B T \, Ln\left(\frac{1}{K} - 1\right) = E_F - E \quad (5)$$

Moreover, K is calculated as follows:

$$K = \frac{\alpha\lambda}{4\pi} \quad (6)$$

where α is the absorption coefficient obtained from UV-Vis spectra. Therefore, plotting K(λ) vs. incident photon energy (hν) and linear fitting of Equation (5) to the linear part of these plots make the calculation of E_F possible [26,27].

According to the model proposed by Tauc and Davis-Mott, light absorption by an amorphous material depends on its optical band gap (E_g) and energy of incident photon (hν) [28,29]. This behavior is represented in Equation (7), as shown in the following:

$$(\alpha h\nu) = \beta^2 (h\nu - E_g)^n \quad (7)$$

where β is a constant and n is an index that exhibits the type of optical transition that takes the values of 2, 3, 1/2, and 1/3 for indirect allowed, indirect forbidden, direct allowed, and direct forbidden transitions, respectively [30-33]. Here, Tauc plots ($(\alpha h\nu)^{1/n}$ vs. hν plots) are employed, and the linear part of these curves is taken into account to compute the band gap energies. In other words, the band gap energy of a glassy material was calculated using the intercept of the linear part of Tau plot divided by its slope.

The disordered structure of amorphous materials is the tailing of electrons density of states into the band gap. The energy of these tails is known as Urbach energy (E_U). Equation (8) shows the relationship between the absorption coefficient and E_U:

$$\alpha = \beta \exp(\frac{h\nu}{E_U}) \quad (8)$$

On the basis of UV-Vis spectra, Ln(α) against hν diagrams can be drawn and E_U can be estimated by least square fitting of Equation (8) to these diagrams [34-37].

2.3.2. Calculation of Refractive Index

The refractive indices of the samples in the UV-Vis region of wavelengths were measured using Fresnel equations (Equations (9) and (10)), reflectance, and transmittance spectra:

$$R = (\frac{N_t - N_i}{N_t + N_i})^2 \quad (9)$$

$$T = (\frac{2N_t}{N_t + N_i})^2 \quad (10)$$

where N_t and N_i are the complex refractive indices of the glass and air, respectively. Moreover, N_t is defined as Equation (11):

$$N = n - iK \quad (11)$$

where K is the extinctions coefficient and n the refractive index. The Reflectance and transmittance spectra of a sample were considered, and a system of two equations and two unknowns was solved by Macleod media, hence the formation of a curve of refractive index vs. wavelength [38,39].

3. RESULTS AND DISCUSSION

3.1. Density, Molar Volume, and Microhardness

Table 1 presents the values of densities and molar volumes of glasses. Incorporation of one mole ratio of Bi_2O_3 decreased the density from 3.84 to 3.74 (g/cm^3); however, higher amounts of Bi_2O_3 increased the density again. In fact, changes in molar mass and molar volume generate variations in density values. As a result of the enhancement of molar mass caused by increasing the Bi_2O_3 content, an increase in the density is required. In contrast, in case Bi_2O_3 plays the role of network modifying, V_m must increase as a consequence of the emergence of more Non-Bridging Oxygens (NBOs) and the density decreases. The calculated value of V_m (Table 1) increase upon adding Bi_2O_3 and approving the network modifying role of this oxide. The effect of V_m outweighs the molar mass in the case of sample GBi1; for other samples, the opposite holds.

Table 1 lists the results from microhardness measurements. Hardness is usually influenced by the introduction of glass network modifiers, which is provoked with the creation of more NBOs and breakup

of the glass network [40]. The decreasing trend of the microhardness of the samples with higher mole ratios of Bi_2O_3 is in accordance with the above-mentioned statement that proves it to some extent.

TABLE 1. Some physical properties of glasses with different amounts of Bi_2O_3

Sample Code	d (g/cm^3)	V_m (cm^3)	Microhardness Hv (MPa)
GBi0	3.84	27.69	720.21
GBi1	3.74	28.41	695.00
GBi2.5	3.77	30.42	677.30
GBi4	3.86	31.05	642.50
GBi6	3.98	31.60	613.10

3.2. Structural Studies

As mentioned in the previous section, Bi_2O_3 acts as a network modifier and affects the glass structure by creating NBOs. To evaluate this claim, FTIR spectra should be studied (Figure 1). All of the samples exhibit three absorption bands at ~440, ~680, and ~970-980 cm^{-1} which are related to rocking, symmetric, and asymmetric stretching vibrations of Si-O-Si bonds, respectively [41]. The wide band with the highest intensity is composed of three over-lapped peaks corresponding to different vibrational modes of Si-O bonds in all silicate units, i.e., Q^n (n=1, 2, 3). The band at 1080-1100 cm^{-1} is generated by stretching vibrations of Si-O bonds with single NBOs (Q^3), and the other one placed at 970-980 cm^{-1} is attributed to the stretching vibration of bonds with two NBOs (Q^2). Finally, the peak at 900-930 cm^{-1}, which is not distinguishable, is created by the stretching vibrations in silicate units with three NBOs (Q^1). Further, Q^1 represents the stretching vibrations of Si-O-Al in aluminosilicate glasses [42,43]. As demonstrated in Figure 1, the position of this broad band shifts to lower wavenumbers from GBi0 to GBi6 and its maximum value is observed at wavenumbers near Q^2 and Q^1 species. Therefore, the number of silicate units with more NBOs grew with the addition of Bi_2O_3. The other band at ~587 cm^{-1} is also related to Si-O-Al asymmetric stretching vibrations [44], and the changes of this band confirm the increase in this type of bonds for samples with Bi_2O_3. Moreover, the broad peak of asymmetric vibrations of Si-O-Si is intensified more than the symmetric vibrations band. All these changes are indicative of the higher numbers of NBOs and disorderliness in the presence of Bi_2O_3 [40].

There are three weak peaks at 1460, 1640, and 1741 cm^{-1} resulting from the vibrations of Al-F bonds [45]. In oxy-fluoride glasses, it is preferred that F^- ions bond to Al^{3+} cations instead of Si^{4+} to decrease the fluorine loss as SiF_4 [46]. Of note, in the spectra of glasses with the exception of GBi6 sample, another weak peak is observed at 534 cm^{-1}, which is probably related to Bi-O bonds. Sample GBi6 lacks this bond mainly because the Bi introduced by six mole ratios of Bi_2O_3 forms Bi° particles (colloidal Bi) instead of Bi-O in this glass, which will be discussed in detail in the next section [47].

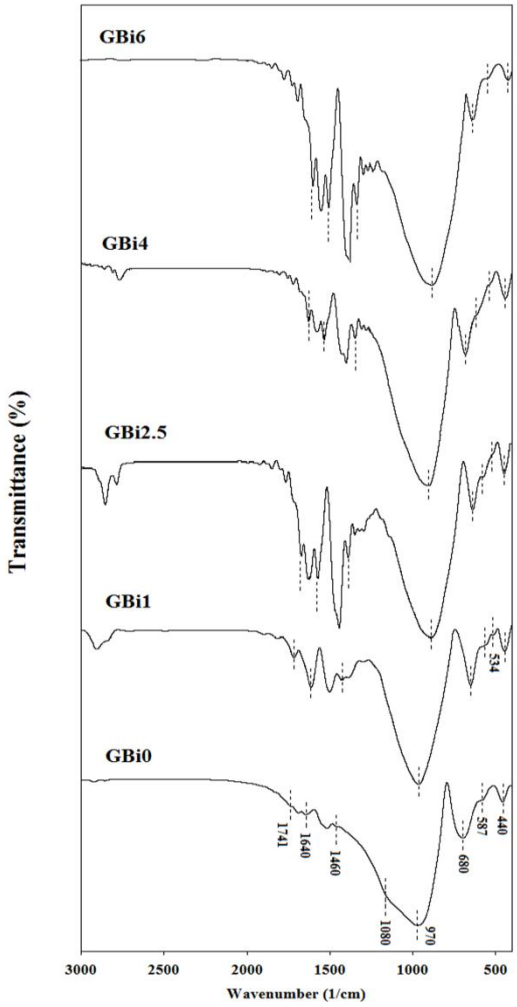

Figure 1. FTIR spectra of glasses containing different amounts of Bi_2O_3

3.3. UV-VIS-IR Transmittance Spectra and Evaluation of Optical Properties

UV-Vis transmittance spectra are plotted in Figure 2. Although there is not any significant difference between the transmittance of samples, their absorption edge has a red-shift to longer wavelengths. Moreover, absorption edges are not sharply defined due to the amorphous nature of the glasses. These absorption edges can be assumed as Urbach fundamental edges [48,49]. A broad absorption peak at ~400-600 nm emerged only for sample GBi6, and it is usually considered as evidence of Bi° particles in glass. In other words, the surface Plasmon resonance of Bi° particles is the reason for this absorption peak [47].

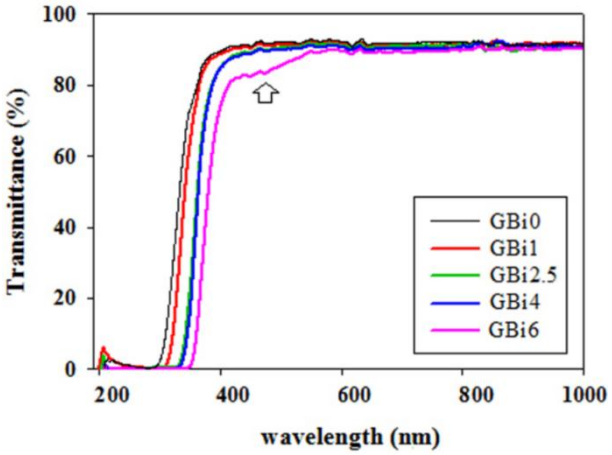

Figure 2. UV-Vis spectra of glasses containing different amounts of Bi_2O_3

Owing to the strong UV absorption rather than visible wavelengths, the extinction coefficient of samples follows Fermi-Dirac distribution function [36], and K(λ) vs. hν plots (Figure 3) are used to calculate Fermi energies, the results of which are demonstrated in Table 2. For this purpose, the linear part of these plots steeping to lower energies was taken into consideration and the formula of the best fitted line to this part was obtained through linear regression analysis. Then, this formula was substituted into Equation (5) and the Fermi energy at each wavelength was calculated. Higher E_F values of glasses compared to k_BT indicate that they are insulators and their insulating behavior varies very slightly to the semiconducting behavior upon adding Bi_2O_3.

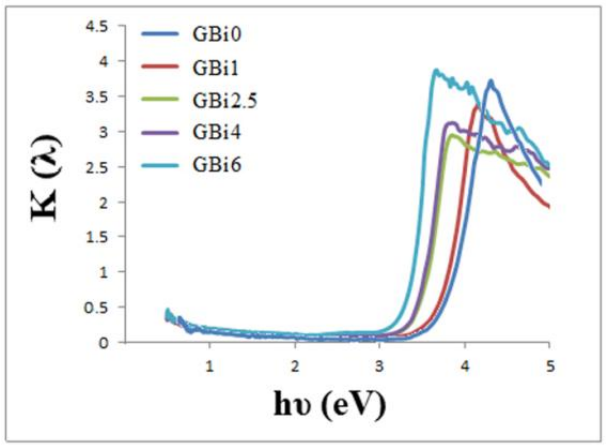

Figure 3. Extinction coefficient vs. energy plots of glasses containing different amounts of Bi_2O_3

Tauc plots of glasses are depicted in Figure 4. The direct and indirect optical band gap energies can be obtained by determining the extrapolation formula of the linear part of these plots and dividing the intercept of this line by its slope. Table 2 includes the values of optical band gaps obtained from these plots. Formation of dangling bonds like NBOs with higher Bi_2O_3 contents reduces the band gap energy by developing the localized states within the band gap and putting the valence and conduction bands closer [50,51].

TABLE 2. Optical properties of oxy-fluoride glasses containing different amounts of Bi_2O_3

Energy (eV) / Sample Code	E_F	$E_{g\ (indirect)}$	$E_{g\ (direct)}$	E_U
GBi0	4.307	3.481	3.950	0.170
GBi1	4.108	3.222	3.752	0.193
GBi2.5	3.805	3.007	3.495	0.204
GBi4	3.759	2.970	3.411	0.209
GBi6	3.649	2.958	3.380	0.212

As stated earlier, in amorphous materials, Urbach tails or the tails of the density of states in forbidden gap spark off the short-range order of these materials. This is the reason why Urbach energy is regarded as a degree of crystallinity and orderliness [50]. To calculate Urbach energies, the slope of the linear part of Ln(α) vs. hν plots (illustrated in Figure 5) is reverted, the results of which are listed in Table 2. In the case of adding Bi_2O_3, Urbach energy increases and this increment is associated with the higher degree of disorderliness caused by increasing the NBOs.

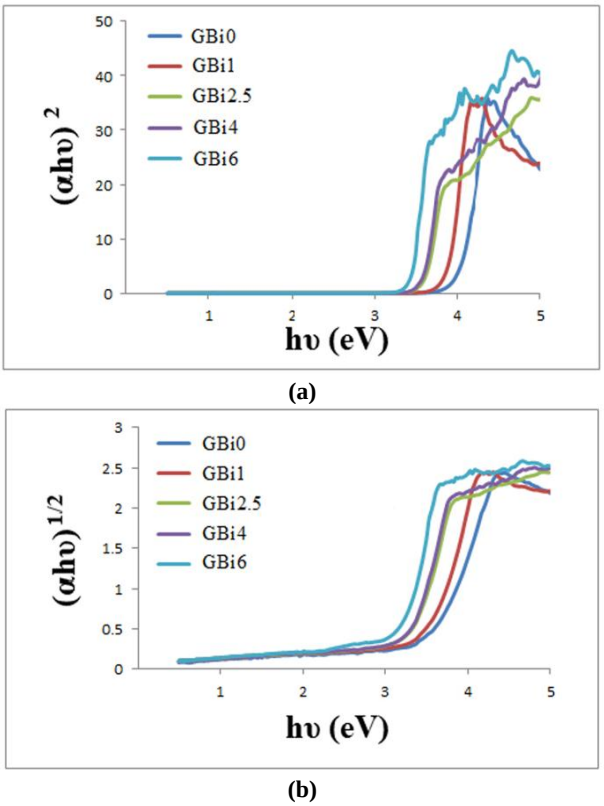

Figure 4. Tauc plots for calculation of (a) direct and (b) indirect band gaps

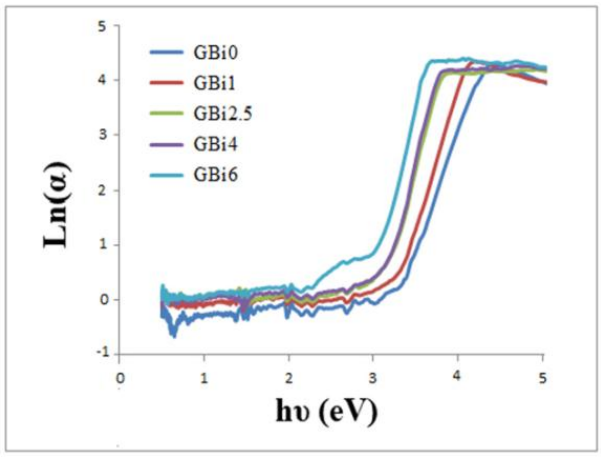

Figure 5. Ln(α) vs. energy diagrams for determination of Urbach energy

Figure 6 illustrates how Bi_2O_3 can affect the IR cut-off position and UV-Vis-IR transmitting window. All of these glasses are transparent in UV-Vis (300-1100 nm) region with transmittance of approximately 90%. In the IR region, the transparencies are acceptable and the IR cut-offs are placed at ~4.7-5 µm. Accordingly, from the IR transmittance point of view, the present glasses can compete with some commercial IR glasses like Schott IRG2 and Schott IR 11 [52].

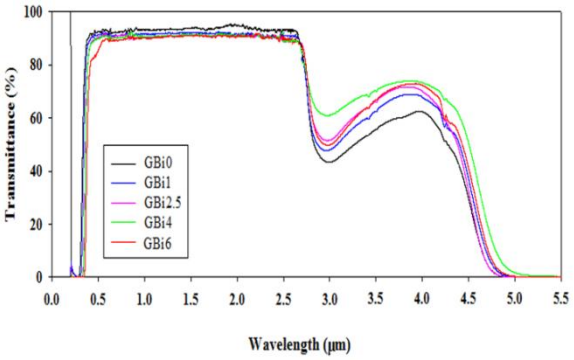

Figure 6. UV-Vis-IR transmittance spectra of glasses containing different amounts of Bi_2O_3

Generally, light absorption in the IR region is different from that in the UV-Vis region of spectrum. Most optical absorptions in the IR region in glasses result from vibrational transitions. The frequency (ν) of a vibrational absorption is given as follows:

$$\nu = (\frac{1}{2\pi})\sqrt{\frac{F}{\mu}} \quad (12)$$

where F is the force constant for bond energy and µ the effective mass [53,54]. According to Section 3.1., the molar mass and number of NBOs increase by introducing Bi_2O_3. Generation of NBOs indicates the F parameter and absorption in the IR region and shifts the IR cut-off to longer wavelengths [37]. However, in case the amount of Bi_2O_3 exceeds four mole ratios, transmittance descents and IR cut-off demonstrate a blue-shift again, mainly due to the light scattering by Bi° particles in GBi6.

The values of the refractive index of glasses as a function of wavelength are presented in Figure 7. In case the quantity of Bi_2O_3 increases, the higher refractive index ensues. In fact, the refractive index of a glass is determined by the interaction of light with electrons of constituent atoms of the glass. In addition, upon increasing the electron density or polarizability of ions, the refractive index would increase. Furthermore, NBOs are more polarizable than bridging oxygens with the ability to increase the refractive index. The polarizability of cations plays a significant role [53]. Of note, the main reasons for such increase in the refractive index include the high polarizability of Bi^{3+} cations and creation of more NBOs.

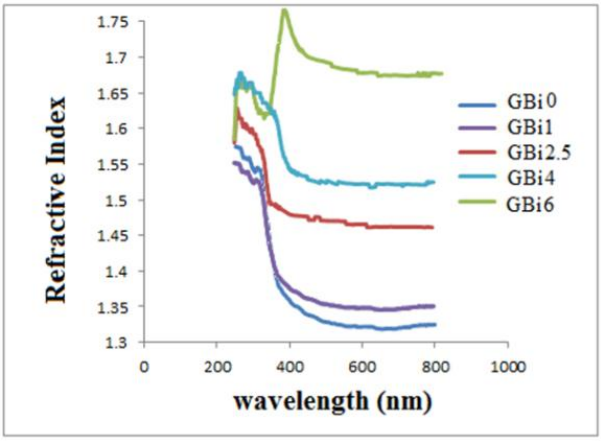

Figure 7. Refractive index curves of glasses containing different amounts of Bi_2O_3

3.4. Crystallization Behavior and Feasibility Study of Transparent Glass-Ceramic Preparation

As reported by other researchers, there are usually two exothermic peaks in the DSC thermo-grams of oxy-fluoride glasses based on BaF_2 [55-57].

In the DSC results of the present glasses (Figure 8), two exothermic peaks are observed. The first peak at lower temperatures is ascribed to the crystallization of BaF_2, and the second one at higher temperatures is related to the crystallization of glassy matrix [58]. According to this figure, the shape of the first peak changes with higher amounts of Bi_2O_3. The crystallization peak of BaF_2 moves to lower temperatures in the presence of Bi_2O_3,

followed by increase in its content since Bi_2O_3 increases the number of NBOs and enhances crystallization. Bocker and Russel [59] proposed a self-organizing model for nano-crystallization of BaF_2 from oxy-fluoride glasses where a highly viscous layer enriched by network former cations was formed that acted a diffusion barrier hindering the crystal growth.

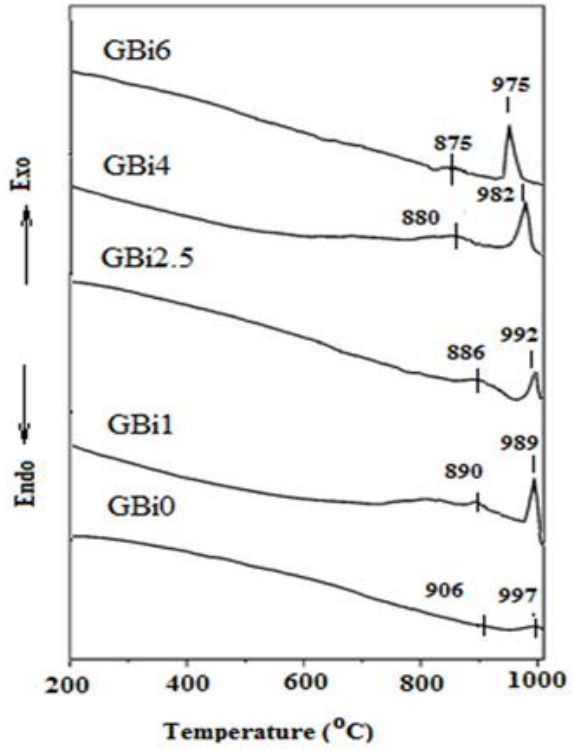

Figure 8. DSC curves of glasses containing various amounts of Bi_2O_3

In case the number of NBOs in oxy-fluoride glasses increased, the residual glassy matrix became less viscous and ions diffused the barrier easier. Therefore, NBOs facilitate the crystallization of BaF_2 and reduce its crystallization temperature [16].

In the XRD patterns of as-made glasses (Figure 9(a)), no diffraction peak is observed since samples are amorphous, hence no unwanted crystallization. Glasses were heat-treated at their first peak temperature for two hours, the XRD patterns of which are depicted in Figure 9(b). Despite the DSC results and our expectations, BaF_2 crystals were not precipitated in samples. Heat-treating at higher temperatures could not solve the problem and apparently, the heat-treated samples lost their transparency. Finally, in glasses crystallized at their second peak temperature, BaF_2 was obtained in company with $BaAl_2Si_2O_8$ (Figure 9(c)).

Hence, it is assumed that crystallization is a surface crystallization process. GBi4 was chosen to justify this possibility, and a fine sample of it was prepared to compare its DSC results with those of the coarse glass sample (Figure 10). The crystallization peak of BaF_2 for the fine sample moved to lower temperature and got sharper, which proved that the crystallization process began from the surface and made it impossible to prepare transparent glass ceramics from the glasses under study. Moreover, hanging the crystallization circumstances has not shown any positive effect on the crystallization of BaF_2 in these glasses and preparation of transparent oxy-fluoride glasses with BaF_2 nanocrystals [60].

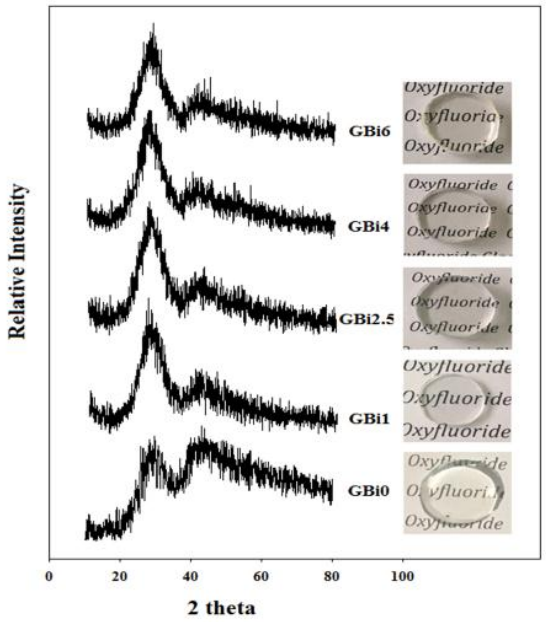

(a)

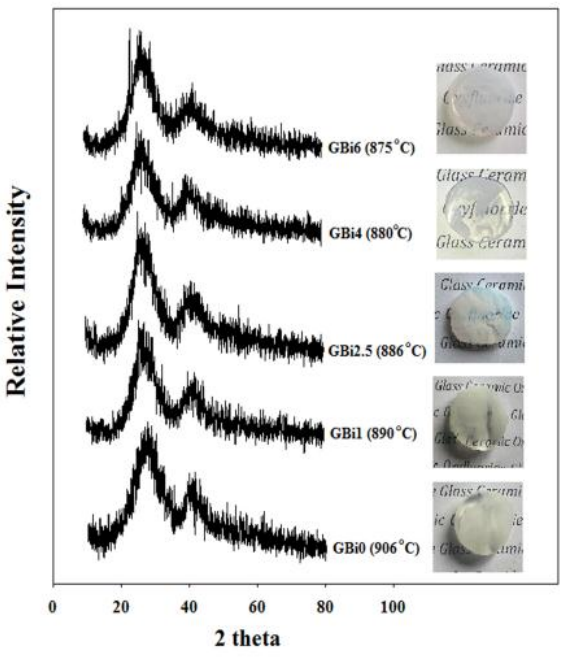

(b)

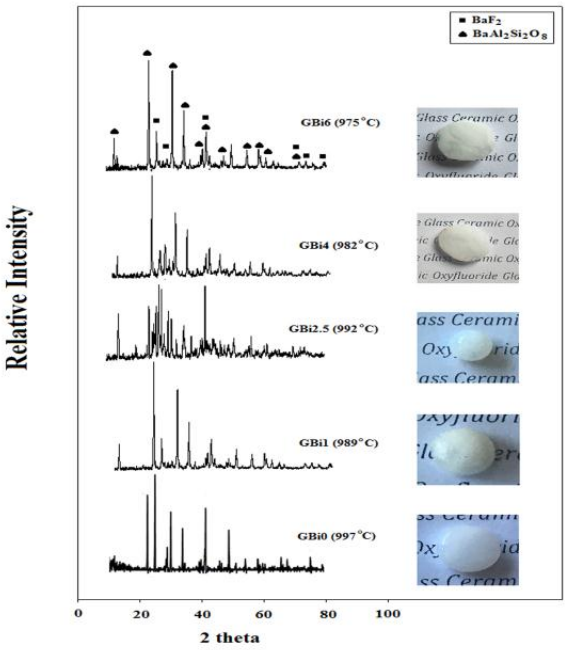

(c)

Figure 9. XRD patterns of (a) as-made glasses and glasses heat-treated at (b) first peak and (c) second peak temperature of DSC results

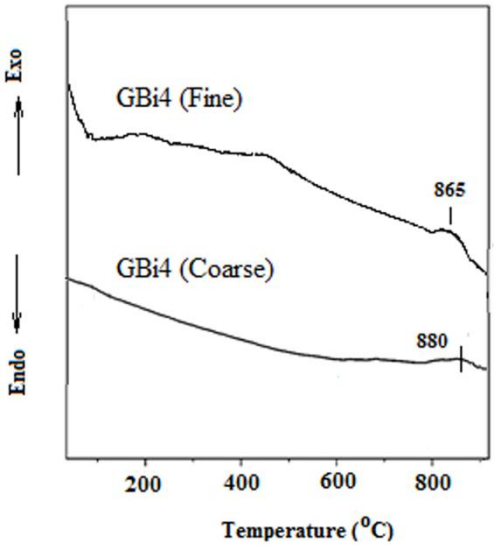

Figure 10. DSC curves of fine and coarse samples of GBi4 glass

4. CONCLUSIONS

- Oxy-fluoride glasses containing different amounts of Bi_2O_3 were prepared using the melt-quenching method. All of the samples were amorphous without any unwanted crystallization as demonstrated by XRD patterns.
- Bi_2O_3 played the role of network modifier, and the value of V_m increased from 27.69 to 31.60 cm^3 for samples GBi0 to GBi6.
- FTIR and UV-Vis spectra proved the presence of Bi° particles in the sample with six mole ratios of Bi_2O_3.
- By adding Bi_2O_3, Fermi energy level and band gap energies decreased and the insulating behavior of glasses was mitigated.
- Urbach energy of sample with more contents of Bi_2O_3 increased from 0.170 to 0.212 eV due to the formation of more NBOs and increment of disorderliness.
- Bi_2O_3 up to four mole ratios increased transmittance and shifted the cut-off to longer wavelengths in IR region.
- In the case of the glass GBi6, refractive index increased to 1.7 due to the higher polarizablility of Bi^{3+} ions and enhancement of NBOs.
- The first exothermic peak in DSC curves related to the crystallization of BaF_2 was moved to lower temperatures due to the creation of more NBOs in the presence of Bi_2O_3. Moreover, transparent glass ceramics were not obtained because of the surface crystallization process.

ACKNOWLEDGEMENTS

We would like to show our gratitude to Ali Rahimian and Laleh Farahinia, our colleagues who provided insight and experties that assisted this research.

REFERENCES

1. Miao, X., Bai, Z., Huo, X., Guo, M., Cheng, F., Zhang, M., "Controllable preparation of CaF_2 transparent glass ceramics: dependence of the light transmittance mechanism on the glass crystallization behaviour", ***Ceramics International***, Vol. 45, No. 7, (2019), 8510-8517. https://doi.org/10.1016/j.ceramint.2019.01.164
2. Gonçalves, M. C., Santos, L. F., Almeida, R. M., "Rare-earth-doped transparent glass ceramics", ***Comptes Rendus Chimie***, Vol. 5, No. 12, (2002), 845-854. https://doi.org/10.1016/S1631-0748(02)01457-1
3. Cai, J., Wei, X., Hu, F., Cao, Z., Zhao, L., Chen, Y., Duan, C., Yin, M., "Up-conversion luminescence and optical thermometry properties of transparent glass ceramics containing CaF_2:Yb^{3+}/Er^{3+} nanocrystals", ***Ceramics International***, Vol. 42, No. 12, (2016), 13990-13995. https://doi.org/10.1016/j.ceramint.2016.06.002
4. Caldiño, U., Bettinelli, M., Ferrari, M., Pasquini, E., Pelli, S., Speghini, A., Righini, G. C., "Rare earth doped glasses for displays and light generation", In Vincenzini, P. (ed.), ***Advances in Science and Technology***, Switzerland: Trans Tech Publications Ltd, Vol. 90, (2014), 174-178. https://doi.org/10.4028/www.scientific.net/AST.90.174
5. Jia, S., Huang, L., Ma, D., Tai, Z., Zhao, S., Deng, D., Wang, H., Jia, G., Hua, Y., Yang, Q., Xu, S., "Luminescence properties of Tb^{3+}-doped oxyfluoride scintillating glasses", ***Journal of***

Luminescence, Vol. 152, (2014), 241–243. https://doi.org/10.1016/j.jlumin.2013.12.036
6. Righini, G. C., Enrichi, F., Zur, L., Ferrari, M., "Rare-earth doped glasses and light Managing in Solar Cells", In ***Journal of Physics: Conference Series***, Mexico, 5–9 November 2018, IOP Publishing Ltd, Vol. 1221, No. 1, (2019), 012028. https://doi.org/10.1088/1742-6596/1221/1/012028
7. Righini, C. G., Ferrari, M., "Photoluminescence of rare-earth-doped glasses", ***La Rivista del Nuovo Cimento***, Vol. 28, No. 12, (2005), 1-53. https://doi.org/10.1393/ncr/i2006-10010-8
8. Kishi, Y., Tanabe, S., "Infrared-to-visible upconversion of rare-earth doped glass Ceramics Containing CaF_2 crystals", ***Journal of Alloys and Compounds***, Vol. 408–412, (2006), 842–844. https://doi.org/10.1016/j.jallcom.2005.01.096
9. Stevenson, A. J., Serier-Brault, H., Gredin, P., Mortier, M., "Fluoride materials for optical applications: single crystals, ceramics, glasses, and glass–ceramics", ***Journal of Fluorine Chemistry***, Vol. 132, No. 12, (2011), 1165–1173. https://doi.org/10.1016/j.jfluchem.2011.07.017
10. Poulain, M., Soufiane, A., Messaddeq, Y., Aegerter, M. A., "Fluoride glasses: synthesis and properties", ***Brazilian Journal of Physics***, Vol. 22, No. 3, (1992), 205-217. http://sbfisica.org.br/bjp/download/v22/v22a24.pdf
11. Polishchuk, S. A., Ignat'eva, L. N., Marchenko, Y. V., Bouznik, V. M., "Oxyfluoride glasses (a review)", ***Glass Physics and Chemistry***, Vol. 37, No. 1, (2011), 1–20. https://doi.org/10.1134/S108765961101010X
12. E1-Mallawany, R., Khafagy, A. H., Ewaida, M. A., Hager, I. Z., Poulain, M. A., Poulain, M. J., "Some physical properties of new oxyfluoride glasses", ***Journal of Non-Crystalline Solids***, Vol. 184, (1995), 141-146. https://doi.org/10.1016/0022-3093(94)00657-1
13. Zhu, L., Lu, A., Zuo, C., Shen, W., "Photoluminescence and energy transfer of Ce^{3+} and Tb^{3+} doped oxyfluoride Aluminosilicate glasses", ***Journal of Alloys and Compounds***, Vol. 509, No. 29, (2011), 7789-7793. https://doi.org/10.1016/j.jallcom.2011.04.154
14. Wang, Y., Ohwaki, J., "New transparent vitroceramics codoped with Er^{3+} and Yb^{3+} for efficient frequency upconversion", ***Applied Physics Letters***, Vol. 63, No. 24, (1993), 3268-3270. https://doi.org/10.1063/1.110170
15. Babu, P., Jang, K. H., Kim, E. S., Shi, L., Seo, H. J., Lopez, F. E., "Optical properties and white-light emission in Dy^{3+}-doped transparent oxyuoride glass and glass ceramics containing CaF_2 nanocrystals", ***Journal of the Korean Physical Society***, Vol. 54, No. 4, (2009), 1488-1491. https://doi.org/10.3938/jkps.54.1488
16. Imanieh, M. H., Eftekhari Yekta, B., Marghussian, V., Shakhesi, S., Martin, I. R.,"Crystallization of nano calcium fluoride in CaF_2-Al_2O_3-SiO_2 system", ***Solid State Sciences***, Vol. 17, (2013), 76-82. https://doi.org/10.1016/j.solidstatesciences.2012.11.008
17. Qiao, X., Fan, X., Wang, M., "Luminescence behavior of Er^{3+} in glass ceramics containing BaF_2 nanocrystals", ***Scripta Materialia***, Vol. 55, No. 3, (2006), 211-214. https://doi.org/10.1016/j.scriptamat.2006.04.023
18. Richman, I., "Longitudinal optical phonons in CaF_2, SrF_2, and BaF_2", ***The Journal of Chemical Physics***, Vol. 41, No. 9, (1964), 2836-2837. https://doi.org/10.1063/1.1726360
19. Zhao, Z., Liu, C., Xia, M., Yin, Q., Zhao, X., Han, J., "Intense ~1.2 μm emission from Ho^{3+}/Y^{3+} ions co-doped oxyfluoride glass-ceramics containing BaF_2 nanocrystals", ***Journal of Alloys and Compounds***, Vol. 701, (2017), 392-398. https://doi.org/10.1016/j.jallcom.2017.01.162
20. Yin, Q., Zhang, J., Liu, C., Xie, J., So, B. J., Heo, J., Zhao, X., "Dual-band photoluminescence of lead selenide quantum dots doped oxyfluoride class-ceramics containing BaF_2 nanocrystals", ***Journal of Non-Crystalline Solids***, Vol. 385, (2014), 136-141. https://doi.org/10.1016/j.jnoncrysol.2013.11.019
21. Chewpraditkul, W., Pattanaboonmee, N., Yawai, N., Chewpraditkul, W., Lertloypanyachai, P., Sreebunpeng, K., Yoshino, M., Liu, L., Chen, D., "Luminescence and scintillation properties of Ce^{3+}-doped SiO_2-Al_2O_3-BaF_2-Gd_2O_3 glasses", ***Optical Materials***, Vol. 98, (2019), 109468. https://doi.org/10.1016/j.optmat.2019.109468
22. Lakshminarayana, G., Qiu, J., "Photoluminescence of Pr^{3+}, Sm^{3+} and Dy^{3+}-doped SiO_2-Al_2O_3-BaF_2-GdF_3 glasses", ***Journal of Alloys and Compounds***, Vol. 476, No. 1-2, (2009), 470-476. https://doi.org/10.1016/j.jallcom.2008.09.015
23. Du, Y., Han, S., Zou, Y., Yuan, J., Shao, C., Jiang, X., Chen, D., "Luminescence properties of Ce^{3+}-doped oxyfluoride aluminosilicate glass and glass ceramics", ***Optical Materials***, Vol. 89, (2019), 243-249. https://doi.org/10.1016/j.optmat.2019.01.018
24. Oo, H. M., Mohamed-Kamari, H., Wan-Yusoff, W. M. D., "Optical properties of bismuth tellurite based glass", ***International Journal of Molecular Sciences***, Vol. 13, No. 4, (2012), 4623-4631. https://doi.org/10.3390/ijms13044623
25. Halimah, M. K., Sidek, H. A. A., Daud, W. M., Zainal, A. S., Mansor, H., Khamirul, A. M., "Physical properties of binary tellurite glass system", ***Solid State Science Technology***, Vol. 18, (2010), 364-370. https://doi.org/10.2109/jcersj1950.86.995_316
26. Khashan, M. A., El-Naggar, A. M., "A new method of finding the optical constants of a solid from the reflectance and transmittance spectrograms of its slab", ***Optics Communications***, Vol. 174, No. 5-6, (2000), 445–453. https://doi.org/10.1016/S0030-4018(99)00721-X
27. El-Kameesy, S. U., Eissa, H. M., Eman, S. A., El-Gamma, Y. A., "Fast neutron irradiation effect on some optical properties of lead borate glass doped with samarium oxide", ***Egyptian Journal of Pure and Applied Science***, Vol. 49, No. 1., (2011), 067-070. https://doi.org/10.21608/ejaps.2011.186253
28. Li, X., Zhu, H., Wei, J., Wang, K., Xu, E., Li, Z., Wu, D., "Determination of band gaps of self-sssembled carbon nanotube films using Tauc/Davis–Mott model", ***Applied Physics A***, Vol. 97, No., 2, (2009), 341–344. https://doi.org/10.1007/s00339-009-5330-z
29. Gautam, C. R., Das, S., Gautam, S. S., Madheshiya, A., Singh, A. K., "Processing and optical characterization of lead calcium titanate borosilicate glass doped with germanium", ***Journal of Physics and Chemistry of Solids***, Vol. 115, (2018), 180–186. https://doi.org/10.1016/j.jpcs.2017.12.038
30. Ghayebloo, M., Rezvani, M., Tavoosi, M., "The relationship between structural and optical properties of Se-Ge-As glasses", ***Infrared Physics and Technology***, Vol. 90, (2018), 40-47. https://doi.org/10.1016/j.infrared.2018.02.004
31. Bavafa, P., Rezvani, M., "Effect of Sn doping in optical properties of Se-Ge glass and glass-ceramics", ***Results in Physics***, Vol. 10, (2018), 777-783. https://doi.org/10.1016/j.rinp.2018.07.021
32. Ibrahim, A., Al-Ani, S K. J., "Models of optical absorption in amorphous semiconductors at the absorption edge-a review and re-evaluation", ***Czechoslovak Journal of Physics***, Vol. 44, No. 8, (1994), 785–797. https://doi.org/10.1007/BF01700645
33. Abdel-Baki, M., Abdel-Wahab, F. A., El-Diasty, F., "One-photon band gap engineering of borate glass doped with ZnO for photonics applications", ***Journal of Applied Physics***, Vol. 111, No. 7, (2012), 073506. https://doi.org/10.1063/1.3698623
34. Shakeri, M. S., Rezvani, M., "Optical properties and structural evaluation of Li_2O-Al_2O_3-SiO_2-TiO_2 glassy semiconductor containing passive agent CeO_2", ***Spectrochimica Acta Part A: Molecular and Biomolecular Spectroscopy***, Vol. 83, No. 1, (2011), 592–597. https://doi.org/10.1016/j.saa.2011.09.009
35. Sayyed, M. I., Rammah, Y. S., Laariedh, F., Abouhaswa, A. S., Badeche, T. B., "Lead borate glasses doped by lanthanum: synthesis, physical, optical, and gamma photon shielding properties", ***Journal of Non-Crystalline Solids***, Vol. 527, (2020), 119731. https://doi.org/10.1016/j.jnoncrysol.2019.119731
36. Khani, V., Alizadeh, P., Shakeri, M. S., "Optical properties of transparent glass-ceramics containing

lithium-mica nanocrystals: crystallization effect", ***Materials Research Bulletin***, Vol. 48, No. 9, (2013), 3579-3584. https://doi.org/10.1016/j.materresbull.2013.05.061

37. Farahinia, L., Rezvani, M., Rezazadeh, M., "Effect of CaF_2 substitution by CaO on spectroscopic properties of oxyfluoride glasses", ***Materials Research Bulletin***, Vol. 139, (2021), 111265. https://doi.org/10.1016/j.materresbull.2021.111265
38. Pedrotti, F. L., Pedrotti, L. M., Pedrotti, L. S., ***Introduction to Optics***, 3rd Ed., Prentice-Hall International, Inc., (1993). http://faculty.du.ac.ir/rajabi/wp-content/uploads/sites/197/2020/09/PEDROTTI-Introduction-to-Optics_3rd.pdf
39. Macleod, H. A., ***Thin-Film Optical Filters***, 4th Ed., Boca Raton, FL: CRC Press, (2010). https://doi.org/10.1201/9781420073034
40. Limbach, R., Karlsson, S., Scannell, G., Mathew, R., Edén, M., Wondraczek, L., "The effect of TiO_2 on the structure of Na_2O-CaO-SiO_2 glasses and its implications for thermal and mechanical properties", ***Journal of Non-Crystalline Solids***, Vol. 471, (2017), 6–18. https://doi.org/10.1016/j.jnoncrysol.2017.04.013
41. Kansal, I., Goel, A., Tulyaganov, D. U., Rajagopal, R. R., Ferreira, J. M., "Structural and thermal characterization of CaO-MgO-SiO_2-P_2O_5-CaF_2 glasses", ***Journal of European Ceramic Society***, Vol. 32, No. 11, (2012), 2739-2746. https://doi.org/10.1016/j.jeurceramsoc.2011.10.041
42. Środa, M., Paluszkiewicz, C., "The structural role of alkaline earth ions in oxyfluoride aluminosilicate glasses-infrared spectroscopy study", ***Vibrational Spectroscopy***, Vol. 48, No. 2, (2008), 246-250. https://doi.org/10.1016/j.vibspec.2008.02.017
43. Mukherjee, D. P., Kumar Das, S., "Effects of nano silica on synthesis and properties of glass ceramics in SiO_2-Al_2O_3-CaO-CaF_2 glass system: A comparison", ***Journal of Non-Crystalline Solids***, Vol. 368, (2013), 98-104. https://doi.org/10.1016/j.jnoncrysol.2013.03.012
44. Farahinia, L., Rezvani, M., Rezazadeh, M., "An investigation into the effects of composition and BaF_2 content on the structure and crystallization behavior of SiO_2-Al_2O_3-K_2O-BaF_2 oxyfluoride glasses", ***Advanced Ceramics Progress***, Vol. 6, No. 1, (2020), 16-21. https://doi.org/10.30501/ACP.2020.105927
45. Snelson, A., "Infrared spectrum of AlF_3, Al_2F_6, and AlF by matrix isolation", ***The Journal of Physical Chemistry***, Vol. 71, No. 10, (1967), 3202-3207. https://doi.org/10.1021/j100869a011
46. Fedorov, P. P., Luginina, A. A., Popov, A. I., "Transparent oxyfluoride glass ceramics", ***Journal of Fluorine Chemistry***, Vol. 172, (2015), 22–50. https://doi.org/10.1016/j.jfluchem.2015.01.009
47. Singh, S. P., Karmakar, B., ***Bismuth oxide and bismuth oxide doped glasses for optical and photonic applications***, (2012). http://cgcri.csircentral.net/1384/1/SPS-Book_Chapter_.pdf
48. Azlan, M. N., Halimah, M. K., Suriani, A. B., Azlina, Y., El-Mallawany, R., "Electronic polarizability and third-order nonlinearity of Nd^{3+} doped borotellurite glass for potential optical fiber", ***Materials Chemistry and Physics***, Vol. 236, (2019), 121812. https://doi.org/10.1016/j.matchemphys.2019.121812
49. Kitamura, N., Fukumi, K., Nakamura, J., Hidaka, T. Hashima, H., Mayumi, Y., Nishii, J., "Optical properties of zinc bismuth phosphate glass", ***Materials Science and Engineering: B***, Vol. 161, No. 1-3, (2009), 91-95. https://doi.org/10.1016/j.mseb.2008.12.023
50. Abdel-Baki, M., El-Diasty, F., Abdel Wahab, F. A. A., "Optical characterization of xTiO_2-(60-x)SiO_2-40Na_2O glasses: II. absorption edge, fermi level, electronic polarizability and optical basicity", ***Optics Communications***, Vol. 261, No, 1, (2006), 65-70. https://doi.org/10.1016/j.optcom.2005.11.056
51. Zhang, X. H., Bureau, B., Lucas, P., Boussard-Pledel, C., Lucas, J., "Glasses for seeing beyond visible", ***Chemistry-A European Journal***, Vol. 14, No. 2, (2008), 432-442. https://doi.org/10.1002/chem.200700993
52. Tang, B., Wu, C., Li, J., Fan, Y., Hu, H., Zhang, L., "Large-size oxyfluoride glasses used for vis-IR-transmitting", ***Journal of Non-Crystalline Solids***, Vol. 355, No. 37-42, (2009), 2006-2009. https://doi.org/10.1016/j.jnoncrysol.2009.01.060
53. Ghayebloo, M., Tavoosi, M., Rezvani, M., "Investigation of comparative effects of antimony and arsenic on the structural and optical behaviors of IR transparent $Ge_{40}Se_{60}$ glass", ***Infrared Physics & Technology***, Vol. 109, (2020), 103387. https://doi.org/10.1016/j.infrared.2020.103387
54. Shelby, J. E., ***Introduction to Glass Science and Technology***, 2nd Edition, Cambridge: Royal Society of Chemistry, (2005). https://doi.org/10.1039/9781847551160
55. Antuzevics, A., Kemere, M., Ignatans, R., "Local structure of gadolinium in oxyfluoride glass matrices containing SrF_2 and BaF_2 crystallites", ***Journal of Non-Crystalline Solids***, Vol. 449, (2016), 29-33. https://doi.org/10.1016/j.jnoncrysol.2016.07.015
56. Sung, Y. M., "Crystallization kinetics of fluoride nanocrystals in oxyfluoride glasses", ***Journal of Non- Crystalline Solids***, Vol. 358, No. 1, (2012), 36-39. https://doi.org/10.1016/j.jnoncrysol.2011.08.016
57. Bocker, C., Wiemert, J., Rüssel, C., "The formation of strontium fluoride nano crystals from a phase separated silicate glass", ***Journal of the European Ceramic Society***, Vol. 33, No. 10, (2013), 1737-1745. https://doi.org/10.1016/j.jeurceramsoc.2013.02.008
58. Huang, L., Jia, S., Li, Y., Zhao, S., Deng, D., Wang, H., Jia, G., Hua, Y., Xu, S., "Enhanced emissions in Tb^{3+}-doped oxyfluoride scintillating glass ceramics containing BaF_2 nanocrystals", ***Nuclear Instruments and Methods in Physics Research A: Accelerators, Spectrometers, Detectors and Associated Equipment***, Vol. 788, (2015), 111-115. https://doi.org/10.1016/j.nima.2015.03.084
59. Bocker, C., Rüssel, C., "Self-organized nano-crystallisation of BaF_2 from Na_2O/K_2O/BaF_2/Al_2O_3/SiO_2 glasses", ***Journal of the European Ceramic Society***, Vol. 29, No. 7, (2009), 1221-1225. https://doi.org/10.1016/j.jeurceramsoc.2008.08.005
60. Haddadi kahnamouei, R., Rezvani, M., "Investigation of Crystallization Behavior of SiO_2-Al_2O_3-BaO-BaF_2 Glass Ceramics", In ***The 12th Congress of Iranian Ceramic Society***, Tehran, 30th April and 1st May 2019, Iran: Iranian Ceramic Society, (2019), 171-179. https://www.dropbox.com/s/t9tbc7hxxxdgb1f/%D9%81%D8%A7%DB%8C%D9%84%20%D9%86%D9%87%D8%A7%DB%8C%DB%8C%20%D9%85%D8%AC%D9%85%D9%88%D8%B9%D9%87%20%D9%85%D9%82%D8%A7%D9%84%D8%A7%D8%AA1.pdf?dl=0